

DOI: 10.1515/amm-2016-0334

K. MIŁKOWSKA - PISZCZEK*[#]

THE EFFECT OF THERMOPHYSICAL PARAMETERS ON TEMPERATURE DISTRIBUTION IN THE PRIMARY COOLING ZONE

The values of thermophysical properties obtained from the experimental research, and those that were calculated with thermodynamic databases, are crucial parameters which were used in the numerical modelling of the steel solidification process. This paper presents the results of research on the impact of specific heat and enthalpy, along with the method of their implementation, on temperature distribution in the primary cooling zone in the continuous steel casting process. A cast slab – with dimensions of 1100 mm and 220 mm and a S235 steel grade – was analysed. A mould with a submerged entry nozzle (SEN), based on the actual dimensions of the slab continuous casting machine, was implemented. The research problem was solved with the finite element method using the *ProCAST* software package. Simulations were conducted using the “THERMAL + FLOW” module.

Keywords: continuous casting of steel, enthalpy, numerical modelling, ProCAST

Nomenclature

c_p - specific heat ($\text{J g}^{-1} \text{K}^{-1}$)
 f_s - solid phase fraction [0-1]
 g - gravitational acceleration
 h - heat transfer coefficient in the mould ($\text{W m}^{-2} \text{K}^{-1}$)
 H - enthalpy (J g^{-1})
 L - latent heat (J g^{-1})
 t - time (s)
 T - temperature (K)
 T_a - ambient temperature (K)
 Q - the heat source term (W m^{-3})
 x, y, z - the 3D coordinate axes
 ρ - density (kg m^{-3})
 σ - Stefan-Boltzmann constant ($\text{W m}^{-2} \text{K}^{-4}$)
 ε - emissivity
 λ - thermal conductivity ($\text{W m}^{-1} \text{K}^{-1}$)
 μ_i - viscosity (Pa s^{-1})
 σ_{ij} - Stokes viscous stress tensor
 δ_{ij} - Kronecker delta

1. Introduction

At present, computing performed on the basis of numerical models is finding more and more application in industrial practice. The application of numerical computing for the analysis and identification of the existing process-related problem can lead to finding an appropriate solution. It results in an improvement of production and the quality of products [1-12]. For the continuous casting of steel, it

could be analysis of the effect of the interaction between the solidifying metal and the mould wall, the effect of the mould powder, or the effect of the non-metallic inclusions. At present the numerical modelling also includes the prediction of cast strand defects such as cracks, porosity or element segregation [3,6]. Many numerical models of the continuous steel casting process used in numerical computations are based upon material parameter average values, i.e. specific heat, viscosity, density [2,12-16]. The use of average values within such a broad temperature range leads to a significant increase in the numerical error concerning the calculated temperature distribution; this is the basis for computing thermal stresses, examining the mould taper, the steel flow within the mould, or predicting cast strand defects.

The thermophysical properties of steel – as determined by experimental research or calculated with thermodynamic databases – are key input parameters for building a numerical model of the continuous casting process. Computing the material parameters of the steel grade tested on the basis of its chemical composition is a common approach [2,8,15-18]. However, it should be emphasised that the temperature distribution obtained with the numerical modelling is extremely sensitive to any changes in the basic thermophysical properties.

2. Thermophysical parameters

The chemical composition is the basic feature that determines the classification of steels. It determines both

* AGH UNIVERSITY OF SCIENCE AND TECHNOLOGY IN KRAKOW, FACULTY OF METALS ENGINEERING AND INDUSTRIAL COMPUTER SCIENCE, AL. MICKIEWICZA 30, 30-059 KRAKÓW, POLSKA

[#] Corresponding author: kamilko@agh.edu.pl

the casting process conditions and the thermophysical and rheological properties of the material tested.

TABLE 1

Chemical composition of S235 steel

| C | Mn | Si | P | S | Cr | Ni | Cu | Al | V | Mo |
|------|-----|------|------|-------|------|------|------|-------|------|------|
| 0.07 | 0.6 | 0.03 | 0.02 | 0.018 | 0.15 | 0.15 | 0.15 | 0.045 | 0.02 | 0.05 |

For the chemical composition of steel S235 presented in table 1 – the following were calculated on the basis of the *CompuTherm LLC* thermodynamic databases supplied together with the *ProCAST* software – enthalpy, heat conductivity, density, viscosity as a function of temperature, as well as the liquidus and solidus temperatures. The *CompuTherm LLC* database engine is based upon models using Gibbs free energy for each phase in the system. The minimum of Gibbs free energy at a given temperature leads to obtaining the phase equilibrium. The Lever algorithm was used – one of three algorithms implemented in the thermodynamic database [19].

2.1. Enthalpy

The relationship between enthalpy and temperature for metal alloys is defined as follows [6,19,20]:

$$H(t) = \int_{T_0}^T c_p(T) dT + (1 - f_s)L \quad T_{sol} \leq T \leq T_{liq} \quad (1)$$

The numerical model of the continuous steel casting process formulated in this paper uses the enthalpy method presented by Equation 1 to calculate temperature distribution. Enthalpy was calculated as a function of temperature using experimental values for the specific heat of steel S235 [6], along with the transformation enthalpy (Enthalpy SH) and thermodynamic databases (Enthalpy DB). The obtained values as a function of temperature were compared and presented in Fig. 1. Enthalpy (DB) was calculated on the basis of the *CompuTherm LLC* thermodynamic databases supplied together with the *ProCAST* software.

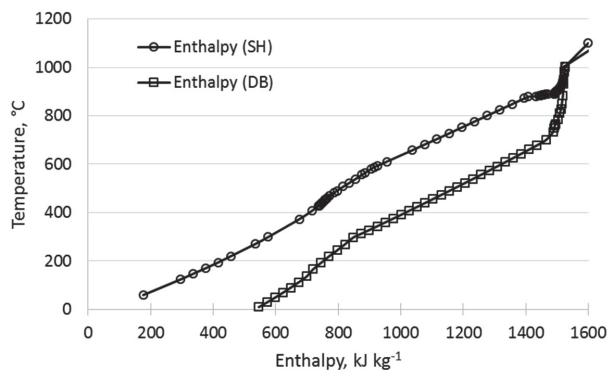


Fig. 1. Enthalpy versus temperature

The biggest difference between the two sets of enthalpy values as a function of temperature was 252 J g^{-1} at a temperature of $950 \text{ }^\circ\text{C}$. It is difficult to apply the values of specific heat as a function of the temperature obtained

by the thermal analysis directly, due to the analysis of transformations occurring in the solidifying alloy [6,21]. Computing the enthalpy value, including, at the right place, the transformation enthalpy, which accompanies the first order phase transformations occurring during the steel solidification, is an additional difficulty.

3. Numerical models of the continuous steel casting process

The numerical model of the steel continuous casting process used for the computing was designed on the basis of the construction of the slab continuous caster at ArcelorMittal Poland's Krakow Branch. A mould with a height of 900 mm and a wall thickness of 40 mm was designed. The mould was assumed to be filled with liquid steel to a constant level of 850 mm. The submerged entry nozzle was designed with a height of 1190 mm, the nozzle port inclination angle of 15° , and the minimum submergence depth during casting of 110 mm. Additionally, the model contained a fragment of the secondary cooling zone, covering three spray zones. Scheme of the mould is presented in Fig. 2.

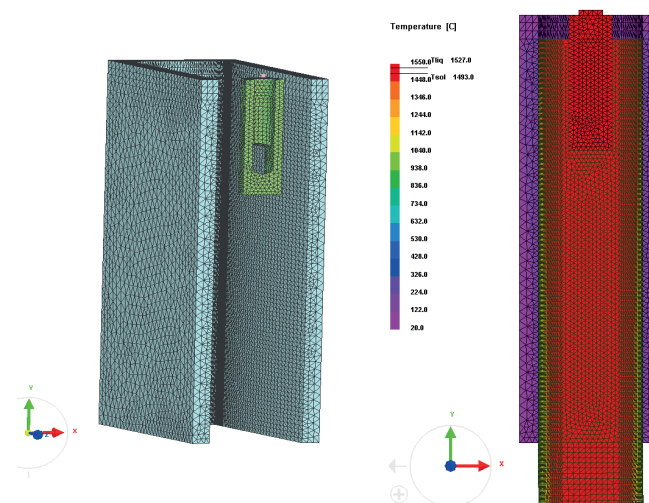


Fig. 2. The mould with submerged entry nozzle

The basic elements of the surface mesh applied on the model were a triangle and a rectangle. 3D mesh elements were generated on the basis of the surface mesh. The finite element mesh contained 1868746 finite elements of various sizes. The smallest mesh elements of 4 mm were designed on the face of the strand contact with the mould wall and in the area of the SEN ports.

3.1. Boundary and initial conditions

In the calculations presented, the heat transfer model was applied in which the temperature field could be determined by solving the Fourier equation [10,20]:

$$\frac{\partial(\rho c_p T)}{\partial t} = \frac{\partial}{\partial x} \left(\lambda \frac{\partial T}{\partial x} \right) + \frac{\partial}{\partial y} \left(\lambda \frac{\partial T}{\partial y} \right) + \frac{\partial}{\partial z} \left(\lambda \frac{\partial T}{\partial z} \right) + Q \quad (2)$$

The solution to the thermal problem is the T vector, which represents the temperature values in the individual nodes of the finite element mesh. In the formulated numerical model of the continuous steel casting process, these boundary conditions may be declared in three various ways. The equation below describes the second- (the Neumann condition) and the third-type boundary conditions:

$$Q = Flux + h(T - T_a) + \sigma\varepsilon(T^4 - T_a^4) \quad (3)$$

A boundary condition related to the heat transfer coefficient of $18000 \text{ W m}^{-2} \text{ K}^{-1}$ was applied on the outer side of the mould. This was intensively cooled with water flowing through channels. For the solidifying strand surface contacting the mould wall, the heat transfer coefficient was calculated as a function of the strand surface temperature. The calculated values were in the range of $860 - 1600 \text{ W m}^{-2} \text{ K}^{-1}$ and have been described in [6]. The heat transfer coefficient achieved its maximum value when the heat was transferred from the liquid steel to the mould. The casting speed of 0.8 m min^{-1} was assumed in the computations.

3.2. Flow model

Apart from the THERMAL module, the FLOW module was used to calculate the temperature distribution in the whole volume of the secondary cooling zone in the numerical computations. The FLOW module activation allowed us to determine a more accurate temperature distribution by taking the liquid steel flow in the SEN area into account. Also the basic flow model based on the Navier-Stokes equation solution was used in the paper [19]:

$$\frac{\partial(\rho\mu_i)}{\partial t} + \frac{\partial}{\partial x_j}(\mu_j\rho\mu_i + p\delta_{ij} - \sigma_{ij}) = \rho g_i \quad (4)$$

4. Results of numerical calculations

The solidifying strand surface temperature in the primary cooling zone was analysed – calculated on the basis of four material data sets:

1. The values of specific heat as a function of temperature coming from the experiment, along with the solidification heat of 113 J g^{-1} – Specific heat (T) [6].
2. The average value of specific heat of $0.68 \text{ J g}^{-1} \text{ K}^{-1}$, along with the solidification heat of 113 J g^{-1} – Specific heat (AVG).
3. The values of enthalpy as a function of temperature calculated on the basis of specific heat value – Enthalpy (SH).
4. The values of enthalpy as a function of temperature calculated on the basis of chemical composition using LCC thermodynamic databases – Enthalpy (DB).

Figure 3 presents the temperature distribution on the surface of the solidifying strand in the mould for the four sets analysed.

The highest values of the solidifying strand surface temperature in the mould were obtained for the Enthalpy (DB), and the lowest values for the Enthalpy (SH) variant. Figure 4 presents the temperature difference between the individual variants for the temperature distribution on the surface of the solidifying strand. The maximum difference in the temperature distribution for the variants based on the values of specific heat [Specific heat (T) and Specific heat (AVG)] was $62 \text{ }^\circ\text{C}$. Note that under 30 cm from the steel level in the mould, the strand surface temperature difference substantially declines. Eventually, at the mould outlet, the strand surface temperature difference was $32 \text{ }^\circ\text{C}$.

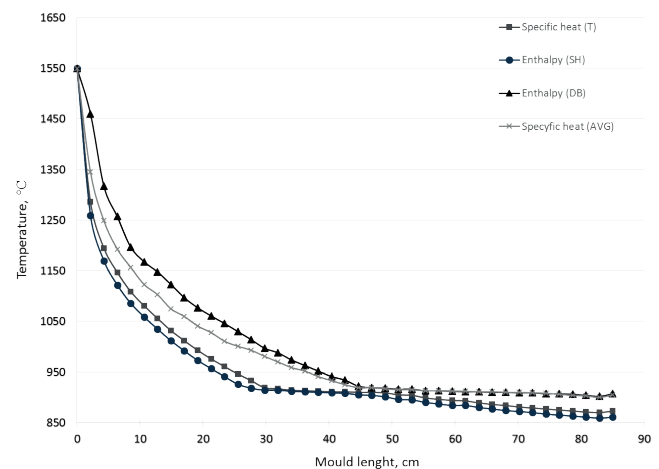


Fig. 3. The temperature distribution along the mould length for all analysed variants

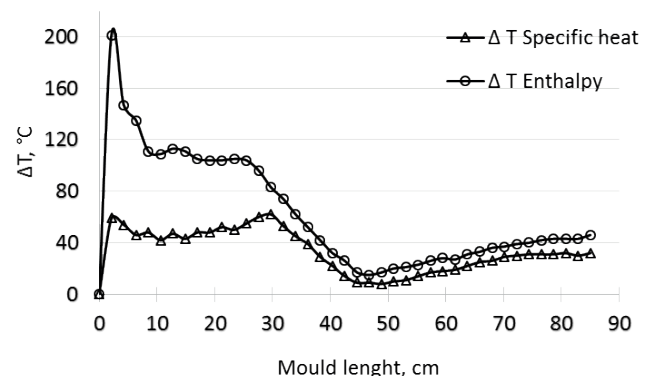


Fig. 4. The temperature differences between the analysed variants along the mould length

The maximum difference in the temperature distribution for the variants based on the enthalpy values ΔT Enthalpy [Enthalpy (SH) and Enthalpy (DB)] was $201 \text{ }^\circ\text{C}$, and the minimum difference was $20 \text{ }^\circ\text{C}$. At the mould exit, the strand surface temperature difference was $46 \text{ }^\circ\text{C}$.

Table 2 presents the shell thickness after leaving the mould for all analysed variants.

TABLE 2

Thickness of the shell after leaving the mould for all variants

| | |
|---------------------|-------|
| Specific heat (T) | 23 mm |
| Specific heat (AVG) | 17 mm |
| Enthalpy (SH) | 25 mm |
| Enthalpy (DB) | 16 mm |

As expected, the smallest shell thickness of 16 mm was obtained for the variant based on the material data coming from the thermodynamic databases. The thickest shell of 25 mm was obtained for the variant based on enthalpy values calculated on the basis of experimental values of specific heat. It should be emphasised that despite the same temperature of the strand surface at the mould exit, different shell thicknesses at the mould outlet were obtained.

5. Summary and conclusions

1. The method of implementation of the values of specific heat and enthalpy in the numerical model of the continuous casting process is key to the correct calculation of the solidifying strand temperature distribution and the prediction of shell thickness.
2. The numerical model of the primary cooling zone allows the sensitivity analysis to be performed for thermophysical parameters and design parameters of the continuous caster.
3. Analysis of findings covered the temperature distribution on the surface of the solidifying strand in the mould and the shell thickness at the time of leaving the mould.
4. The maximum difference in the temperature distribution for the variants examined was 201 °C.
5. The maximum difference in the shell thickness for the variants examined was 9 mm.
6. The formulated model may be used for testing the design and submergence depth of the SEN.

Acknowledgements

This research work was financed through statutory funds at AGH University of Science and Technology 11.11.110.293

REFERENCES

- [1] B.G. Thomas, L. Zhang, *Metallurgical and Materials Transactions B* **33B**, 795 – 812 (2002).
- [2] D. Mazumdar, J.W. Evans, *Modeling of steelmaking process*, CRC Press, New York, (2010).
- [3] K. Vollrath, *Stahl und Eisen* **133**, 45-53, (2013).
- [4] M. Warzecha, T. Merder, *Metalurgija* **52**, 153-156 (2013).
- [5] J. Jezierski, Z. Buliński, K. Janerka, M. Stwarz, K. Kaczmarek, *Indian Journal of Engineering and Materials Sciences* **21**, 322-328 (2014).
- [6] K. Miłkowska-Piszczyk, J. Falkus, *Archives of Metallurgy and Materials* **60**, 1, 251- 256 (2015).
- [7] A. Cwudziński, J. Jowsa, *Archives of Metallurgy and Materials* **57**, 1, 297-301 (2012).
- [8] A. Burbelko, J. Falkus, W. Kapturkiewicz, K. Sołek, P. Drozd, M. Wróbel, *Archives of Metallurgy and Materials* **57**, 1, 379-384 (2012).
- [9] A. Cwudziński, *Steel Research International* **85**, 4, 623-631 (2014).
- [10] Z. Malinowski, M. Rywotycki, *Archives of Civil and Mechanical Engineering* **9**, 59-73 (2009).
- [11] A. Cwudziński, *Archives of Metallurgy And Materials* **56**, 1, 611-618 (2012).
- [12] J. Sengupta, B.G. Thomas, M.A. Wells, *The use of water cooling during the continuous casting of steel and aluminum alloys*, *Metallurgical and Materials Transaction A* **36A**, 187-204 (2005).
- [13] L.-G. Zhu, R.V. Kumar, *Ironmaking and Steelmaking* **34**, 1, 76-82 (2007).
- [14] B.G. Thomas, *Iron and Steel Technology* **7**, 70-87 (2010)
- [15] R. Chaudhary, B.G. Thomas, S.P. Vanka, *Metallurgical and Materials Transactions B* **43B**, 3, 532-553 (2012).
- [16] R. Singh, B.G. Thomas, S.P. Vanka, *Metallurgical and Materials Transactions B* **45B**, 3, 1098-1115 (2014).
- [17] M. Tkadleckova, K. Gryc, P. Machovcak, P. Klus, K. Michalek, L. Socha, M. Kovac, *Materiali in Tehnologije* **46**, 4, 399-402 (2012)
- [18] K. Michalek, K. Gryc, M. Tkadleckova, D. Bocek, *Archives of Metallurgy and Materials* **57**, 1, 291-296 (2012).
- [19] ProCAST 2015, User manual
- [20] J. Falkus, K. Miłkowska-Piszczyk, *Materiali in Tehnologije* **49**, 6, 903-912 (2015).
- [21] E. Wielgosz, T. Kargul, J. Falkus, *Comparison of experimental and numerically calculated thermal properties of steels*. In: *Proceedings paper, METAL 2014: 23rd International Conference on Metallurgy and Materials*, Brno 2014.